Journal of Materials Chemistry C

ROYAL SOCIETY OF CHEMISTRY

REVIEW

View Article Online
View Journal | View Issue

Cite this: J. Mater. Chem. C, 2022, 10, 4521

Intermolecular TADF: bulk and interface exciplexes

Jiannan Gu,[a] Zhenyu Tang,[a] Haoqing Guo,[a] Ye Chen,[a] Jing Xiao,*[b] Zhijian Chen*[a] and Lixin Xiao *[a]

As intermolecular excited states with separated HOMO and LUMO, exciplexes for OLED are gradually taking a contribution in thermally activated delayed fluorescent (TADF) devices due to their advantages in triplet exciton utilization and charge balance. Since Adachi found TADF properties from intermolecular exciplex systems in 2012, a variety of exciplexes containing donors and acceptors have been developed to show TADF characters. In addition to the use of triplet exciton emission through TADF exciplexes for emitters to achieve a high EQE, exciplexes can also be used as hosts of emitters to extend the device lifetime by decreasing the triplet exciton concentration and improving the charge balance, which delays degradation and aging of organic molecules. In this paper, TADF exciplexes are discussed and summarized by dividing into bulk and interface types. The bulk type can generate exciplexes more stably, whether acting as emitters or hosts, which has been widely reported. The interface exciplex TADF has a shorter development time than that of the bulk type, but shows greater potential. The excitons generated by the interface-type exciplex are concentrated at the interface of the donor/acceptor molecules, and the recombination zone is about 5 nm thick, which can effectively reduce the exciton capture by transport materials, leading to higher efficiency and better stability.

Received 15th October 2021,
Accepted 29th January 2022

DOI: 10.1039/d1tc04950j

rsc.li/materials-c

1. Introduction

In the past few decades, research on organic light-emitting diodes (OLEDs) has made tremendous progress.[1–3] In an OLED, electrons and holes are injected from the negative and positive electrodes, and pass through the electron transport layer (ETL) and hole transport layer (HTL), respectively, to form electron–hole pairs in the light-emitting layer (EML), namely, excitons. According to the law of spin statistics, the ratio of the number of excitons in the spin singlet state (S_1) to the triplet state (T_1) is 1 : 3,[4] and the excitons in the triplet state cannot radiate to the ground state due to spin-forbidden resistance. For traditional fluorescent OLEDs, the internal quantum efficiency (IQE) will not exceed 25%.[5] Therefore, effectively using triplet excitons is the key to improve the efficiency of OLEDs.

At present, the most common method of using triplet excitons is to use phosphorescent materials. Phosphorescent materials are

[a] State Key Laboratory for Artificial Microstructures and Mesoscopic Physics, Department of Physics, Peking University, Beijing 100871, P. R. China. E-mail: lxxiao@pku.edu.cn, zjchen@pku.edu.cn
[b] College of Physics and Electronic Engineering, Taishan University, Taian, Shandong 271000, P. R. China. E-mail: xiaojingzx@163.com

Jiannan Gu

Jiannan Gu is a PhD student at the Department of Physics, Peking University. He received his bachelor's degree from Peking University in 2017. His research focuses on organic optoelectronic devices.

Zhenyu Tang

Zhenyu Tang is a PhD student at the Department of Physics, Peking University. He received his master's degree from Shanghai University in 2019. His research focuses on organic optoelectronic devices.

usually complexes containing heavy metal atoms such as iridium or platinum. The spin–orbit coupling effect of heavy atoms enhances the possibility of radiation from the triplet state to the ground state of phosphorescent materials, thus achieving the upper limit of 100% IQE.[6–8] However, phosphorescent materials are expensive because they usually contain precious metal elements, and the efficiency roll-off problem is more serious, especially for blue emission. When the energy level difference between the triplet and the singlet (ΔE_{ST}) is very small ($\sim k_bT$), under the disturbance of thermal motion, the triplet exciton will cross the intersystem crossing (RISC) to the singlet exciton state, and then transit back to the ground state to give a radiation. This process is called thermally activated delayed fluorescence (TADF). In the TADF process, the theoretical maximum IQE may reach 100%.[9–11]

According to the quantum chemistry theory, the energy of S_1 and T_1 of a molecule can be expressed as follows:[12]

$$E_S = E + K + J \quad (1)$$

$$E_T = E + K - J \quad (2)$$

In the formula, E is the orbital energy, K is the electron repulsion energy, and J is the electron exchange energy. ΔE_{ST} can be expressed as follows:

$$\Delta E_{ST} = E_S - E_T = 2J \quad (3)$$

J is proportional to the degree of overlap of the highest occupied molecular orbital (HOMO) and the lowest unoccupied molecular orbital (LUMO) of the molecule. To obtain a small ΔE_{ST}, it is necessary to separate the HOMO and LUMO of the molecule as much as possible to reduce J.

For intramolecular TADF, the HOMO and LUMO orbitals are spatially separated by introducing electron donating and withdrawing groups. Recently, there has also been a new molecular design of TADF: multiple resonance TADF. This type of molecule uses the combination of boron and nitrogen atoms (B–N) to cause the opposite resonance effect. The former attracts the cloud of electrons to its neighbours, and the latter pushes electrons away. The benefits of multi-resonance-induced TADF molecules include not only strong oscillation intensity and high quantum yield, but also significantly better colour purity,[13] and these emitters play an important role in blue TADF.

While the separated HOMO and LUMO orbitals can also be achieved by intermolecular excited states: exciplex, which is a kind of bimolecular complex formed between the ground-states of donors and excited-states of acceptors. As shown in Fig. 1, two different molecules are attracted to each other by the coulombic effect and then charge transfer (CT) occurs between them to form a transient excited state. The exciplex is generally formed between strong electron donors and acceptors. Due to the potential barrier between the interfaces of the two molecules, a large number of electrons and holes accumulate at the interface; finally, the electrons transition from the LUMO

Haoqing Guo

Haoqing Guo is a PhD student at the Department of Physics, Peking University. He received his master's degree from Jilin University in 2017. His research focuses on organic optoelectronic materials.

Jing Xiao

Jing Xiao received her PhD degrees from Beijing Jiaotong University in 2007. In 2017, she became a professor where she founded and chaired the Institute of Photoelectric Information Materials and Devices. Her research interests include organic photoelectric materials and devices.

Zhijian Chen

Zhijian Chen is a full professor at the Department of Physics, Peking University. He received his PhD from the Tokyo University of Agriculture and Technology in 2002. He has been working on OLEDs and solar cells.

Lixin Xiao

Lixin Xiao is a full professor at the Department of Physics, Peking University. He is an RSC Fellow. He received his PhD from the University of Tokyo in 2000. He has been working on OLEDs and solar cells.

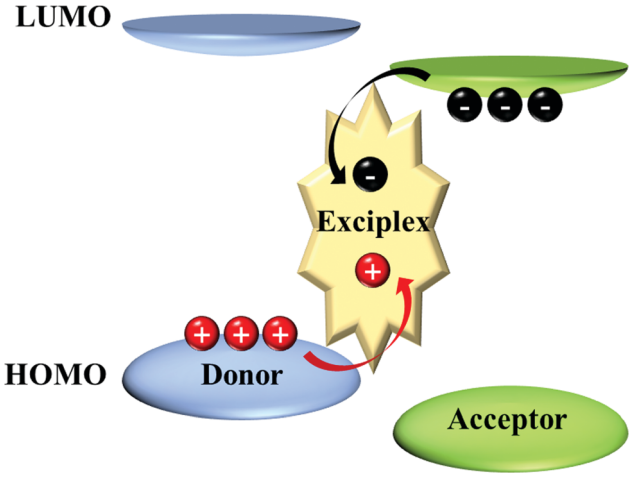

Fig. 1 Concept scheme of the intermolecular exciplex.

of the accepting molecule to the HOMO of the donor, forming the excitons. More detailed introduction about the mechanism of exciplex formation and emission has been previously reviewed.[14–19] In the exciplex, since the CT occurs between two molecules, it naturally satisfies the separation of HOMO and LUMO, resulting in a small ΔE_{ST}, which is a favourable TADF system.

Compared with intramolecular TADF, the intermolecular TADF has its unique advantages: (a) a large number of exciplex candidates can be easily generated by simply combining suitable commercial electron and hole transport materials; there is no need for complex synthesis. (b) The bipolarity of the emission layer increases the charge transport capability, since traditional host materials have a problem of poor charge balance. In addition, bipolar hosts composed of electron and hole transport materials can solve this problem and improve the quantum efficiency of the device.

The existence of exciplex is a normal case in the OLED, but it has been considered as an unfavourable factor for reducing colour purity or used to adjust luminescence peaks. Until 2012, Adachi *et al.* proposed that the RISC process of the exciplex can be effectively used to harvest triplet excitons, breaking through the 25% upper limit of fluorescence IQE. They found that in the 4,4′,4″-tris(*N*-3-methylphenyl-*N*-phenylamino)triphenylamine (m-MTDATA):tris-[3-(3-pyridyl)mesityl]borane (3TPYMB) system, although its photoluminescence quantum yield (PLQY) was only 26%, the external quantum efficiency (EQE) reaches 5.4%, indicating that a high triplet utilization rate (54.2% of delayed fluorescent component) was achieved.[20]

2. Bulk exciplex TADF

The bulk exciplex is mixed with donors and acceptors to form a complex, and we introduce these exciplexes according to the emission colour as follows:

2.1 Bulk exciplexes for green emission

Green emission exciplexes are the earliest developed exciplex system. In 2012, based on the original system, Adachi used 2,8-bis(diphenyl phosphoryl)dibenzo-[*b*,*d*]thiophene (PPT) as the acceptor to form a m-MTDATA:PPT exciplex, and got a maximum EQE of 10% and a power efficiency (PE) of 47 lm W^{-1} for the device.[20] In 2015, Cheah *et al.* used a mixture of tris(4-carbazoyl-9-ylphenyl)amine (TCTA) and 2,4,6-tris(3′-(pyridin-3-yl)biphenyl-3-yl)-1,3,5-triazine (Tm3PyBPZ) to fabricate a green (514 nm) device with a structure of ITO/HAT-CN (5 nm)/TAPC (55 nm)/TCTA : Tm3PyBPZ (1 : 1) (30 nm)/Tm3PyBPZ (40 nm)/Liq/Al, where ITO is indium tin oxide, HAT-CN is 1,4,5,8,9,11-hexaazatriphenylenehexacarbonitrile, TAPC is 1,1-bis(4-(*N*,*N*-di(*p*-tolyl)-amino)phenyl)cyclohexane as the HTL, Liq (8-hydroxyquinolinato lithium) is the ETL. The time-resolved spectrum shows an instantaneous and delayed fluorescent component, which indicates the formation of the TADF exciplex, the maximum EQE is 13.1%, and the turn-on voltage is as low as 2.4 V.[21] In 2016, Hung *et al.* reported another exciplex system. He combined the HT material (HTM) of 9,9′,9″-triphenyl-9*H*,9′*H*,9″*H*-3,3′:6′,3″-tercarbazole (Tris-PCz) with a trimer molecule of 3′,3‴,3⁗-(1,3,5-triazine-2,4,6-triyl)tris(([1,1′-biphenyl]-3-carbonitrile)) (CN-T2T) as the receptor, a green emission (530 nm) was obtained with a maximum EQE of 11.9% (current efficiency (CE) 37 cd A^{-1}, PE 46.5 lm W^{-1}) by using a structure of ITO/4 wt% ReO_3:Tris-PCz (60 nm)/Tris-PCz (15 nm)/Tris-PCz : CN-T2T (1 : 1) (25 nm)/CN-T2T (50 nm)/Liq/Al. Although TCTA has a higher hole mobility than that of Tris-PCz, the device EQE of TCTA drops 16%. It can be seen that the balance of charge transport is crucial to the device efficiency.[22] Li *et al.* used m-MTDATA as the donor and 4,7-diphenyl-1,10-phenanthroline (Bphen) as the acceptor, and the device structure was ITO/m-MTDATA (27 nm)/m-MTDATA:70 mol% Bphen (23 nm)/Bphen (20 nm)/8-hydroxyquinoline aluminium salt (Alq_3) (13 nm)/LiF/Al, a maximum EQE of 7.8% was obtained. In order to study the factors that limit the device efficiency, they also analysed the transient electroluminescence (EL) spectrum of the device. The results indicated that the quenching caused by unbalanced charge transport is an important reason for the reduced luminous efficiency.[23]

Exciplex systems with a high quantum efficiency should meet the following conditions: (a) enough energy level difference between the donor and the acceptor molecules to ensure effective formation of intermolecular excited states; when the HOMO and the LUMO energy levels of donor are different from those of the acceptor by more than 0.4 eV,[15] the exciplex can be formed stably. (b) Donor and acceptor molecules should have higher E_T than that of the formed exciplex, to avoid the efficiency drop caused by the reverse energy transfer of excitons. Since the E_T of the exciplex is close to the singlet energy level, the E_T value of the donor and acceptor molecules is required to be at least close to or reach the singlet energy level of the formed exciplex ($E_{exciplex}$), which can be predicted by the redox potentials of constituting molecules:

$$E_{exciplex} = e(E_{ox,D} - E_{red,A}) + \text{constant}$$

where $E_{ox,D}$ and $E_{red,A}$ are the oxidation potential of the donor and the reduction potential of the acceptor, respectively; the value of the constant in this equation ranges from 0 to 0.2 eV.[24]

Furthermore, the emission mechanism of the exciplex was broadly studied. In 2016, Monkman *et al.* used

m-MTDATA:2,2′,2″-(1,3,5-benzinetriyl)-tris(1-phenyl-1-*H*-benzimidazole) (TPBi), *N*,*N*′-bis(3-methylphenyl)-*N*,*N*′-diphenylbenzidine (TPD):TPBi, TPD:1,3-bis[2-(4-*tert*-butylphenyl)-1,3,4-oxadiazo-5-yl]-benzene (OXD-7) exciplex systems to specifically study the exciton luminescence mechanism, and confirmed that in the small ΔE_{ST} system, the main utilization of triplet excitons resulted from the RISC process, *i.e.*, TADF, while in the large ΔE_{ST} system, the triplet–triplet annihilation (TTA) process makes the dominant contribution.[25] Subsequently, Monkman *et al.* used the m-MTDATA:3TPYMB system to study the influence of an external electric field on the luminescence of the exciplex. When electrons and holes are more tightly bound, the radiation transition is enhanced. He compared two devices: ITO/PEDOT:PSS (40 nm)/m-MTDATA : 3TPYMB 1 : 1 (30 nm)/3TPYMB (30 nm)/LiF/Al and ITO/PEDOT:PSS (40 nm)/m-MTDATA (30 nm)/3TPYMB (30 nm)/LiF/Al, the device performance of the bulk type is significantly higher than that of the interface one.[26] The mixed layer makes more sufficiently for the formation of exciplexes. In 2017, Hu *et al.* studied the effect of the molar ratio of donor and acceptor molecules on the efficiency of exciplex. They used an exciplex system of m-MTDATA:OXD-7, and the highest exciton utilization rate reached 74.3% with 1 : 1 of donor : acceptor ratio and the EQE was 3.8%.[27]

For bulk exciplexes, the spatial structure between molecules has an important influence on the final radiation efficiency. In 2021, Zheng *et al.* suppressed the non-radiative transition of emitters by introducing the intermolecular hydrogen bond, thereby improving their efficiency and stability. With intermolecular hydrogen bond, 13PXZB:B4PyMPM shows the highest PLQY (69.6%) and the lowest rate constant of the non-radiative process of triplet excitons.[28] Besides, they synthesized two donors of 10,10′-(pyridine-2,4-diyl) bis(9,9-dimethyl-9,10-dihydroacridine) (Pra-2DMAC) and 10,10′-(pyrimidine-2,4-diyl) bis(9,9-dimethyl-9,10-dihydroacridine) (Prm-2DMAC), Pra-2DMAC with a vertical configuration exhibited great molecular stability and rigid structure. Prm-2DMAC with a near-planar configuration weakens the electron-donating ability and resulted in an increased overlap of HOMO and LUMO, because the molecule structure was distorted, which has a negative effect on the exciplex performance. The Pra-2DMAC:2,4,6-tris[3-(diphenylphosphinyl)phenyl]-1,3,5-triazine (PO-T2T)-based device showed a maximum EQE of 15.0%, a low roll-off at 1000 cd m^{-2} (EQE 13.9%) and a low turn-on voltage of 2.4 V.[29]

Exciplex can not only be directly used as an emitter, but also as a host. Zhang *et al.* used the fluorescent dopant 2,3,6,7-tetrahydro-1,1,7,7-tetramethyl-1*H*,5*H*,11*H*-10-(2-benzothiazolyl) quinolizino-[9,9*a*,1*gh*] coumarin (C545T) to prepare a green OLED, using the exciplex host of 1,1-bis[4-[*N*,*N*-di(p-tolyl) amino]phenyl]cyclohexane (TAPC):3-(4,6-diphenyl-1,3,5-triazin-2-yl)-9-phenyl-9*H*-carbazole (DPTPCz), which is very close to the HOMO and LUMO energy levels of C545T, to reduce the exciton trapping. Controlling the dopant at a lower concentration to reduce TTA with a structure of device: ITO/TAPC (40 nm)/TAPC:DPTPCz:*x* wt% C545T (30 nm)/1,3,5-tri[(3-pyridyl)-phen-3-yl] benzene (TmPyPB) (50 nm)/LiF/Al, the highest EQE of 14.5% is achieved when doped with 0.2 wt% of C545T, and the turn-on voltage is 2.8 V. The device efficiency is only 3.9% with a non-TADF complex as the host. It can be inferred that the IQE of the exciplex system is close to 100%.[30] In 2014, Kim *et al.* reported a green OLED with an EQE up to 29.6%. The device structure is ITO (70 nm)/(4 wt% ReO_3):mCP (50 nm)/mCP (15 nm)/mCP:bis-4,6-(3,5-di-3-pyridylphenyl)-2-methylpyrimidine (B3PYMPM):5 wt% (4s,6s)-2,4,5,6-tetra(9*H*-car-bazol-9-yl) isophthalonitrile (4CzIPN) (30 nm)/B3PyMPM (20 nm)/(4 wt% Rb_2CO_3):B3PyMPM (35 nm)/Al, with a turn-on voltage of 3.0 V[31] and a maximum CE of 95.5 cd A^{-1}. In 2020, Wei *et al.* reported a series of electron acceptors with TAPC blend films as the EML to exhibit low driving voltages of 2.6–3.0 V for 100 cd m^{-2} and 3.1–4.2 V for 1000 cd m^{-2}. By doping with tris(2-phenylpyridine)iridium ($Ir(ppy)_3$), one of them shows the highest EQE of 29.6%,[32] and the EQE can be maintained at 27.4% at 5000 cd m^{-2}.

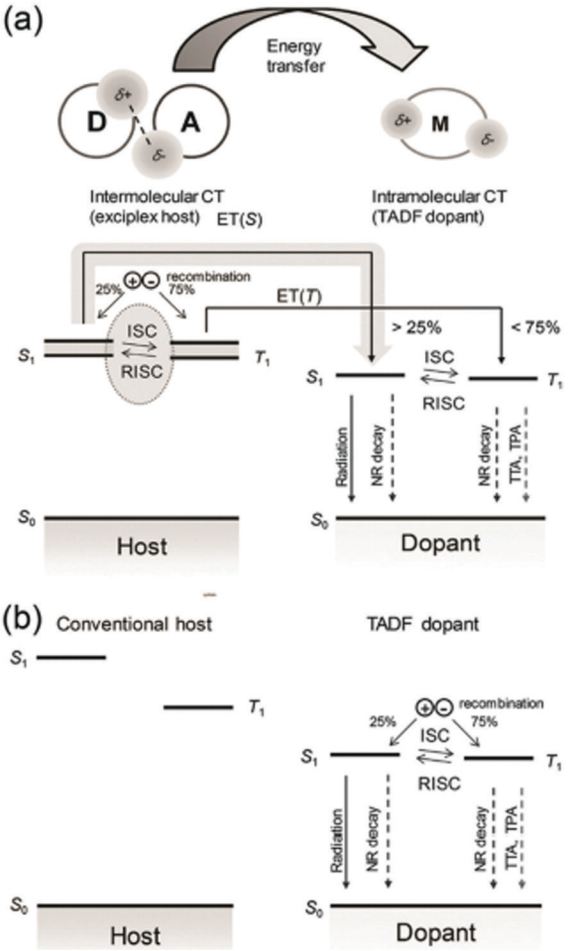

Fig. 2 (a) Schematic concept of combined inter- and intramolecular charge-transfer processes for fluorescent OLEDs. Processes are shown using arrows, with broken arrows representing nonradiative decay. The exciplex states are shown as energy bands to express the distribution of energy levels. Charge recombination in the exciplex host, ISC, and RISC processed on the exciplex, and Förster resonance energy transfer (FRET) to the dopant increases the singlet ratio of the TADF dopant than 25%. (b) Recombination and emission in a conventional host–TADF dopant system. The recombination takes place mostly on TADF dopant molecules *via* trap-assisted recombination and only 25% of singlet excitons are initially generated on the dopant. Reproduced with permission from ref. 33. Copyright 2017, Wiley-VCH.

In OLED, an important unfavorable factor that causes device aging and efficiency roll-off is the high concentration of triplet excitons. When the exciplex is used as the host, whether it is doped with general fluorescent or TADF guest, compared with other non-TADF hosts, it provides another way for triplet excitons *via* RISC, effectively shorting the lifetime of triplet excitons in the EML, *i.e.*, reducing the concentration of triplet excitons,[33] the schematic concept of combined inter- and intramolecular charge-transfer processes for fluorescent OLEDs is shown in Fig. 2(a).

Compared with the conventional hosts (as shown in Fig. 2(b)), the efficiency roll-off of TADF materials doped in the exciplex host is suppressed. Kim *et al.* compared the results of 9-[4-(4,6-diphenyl-1,3,5-triazin-2-yl) phenyl]-*N*,*N*,*N*,*N*′-tetraphenyl-9*H*-carbazole-3,6-diamine (DACT-II) doped with TCTA:B3PYMPM or 4,4′-bis(carbazol-9-yl) biphenyl (CBP) as the host, respectively. Not only does the exciplex host device have a higher maximum EQE (34.2% : 29.6%), as the brightness increases, but the efficiency roll-off was also greatly improved.

In order to further reduce the working voltage of the device and improve the power efficiency, Kido *et al.* compared several ETMs with CBP to form exciplex: 2-phenyl-4,6-bis(3,5-di-4-pyridylphenyl) pyrimidine (B4PyPPM), 4,6-bis(3,5-di(pyridin-4-yl) phenyl)-2-methylpyrimidine (B4PyMPM), 4,6-bis(3,5-di(pyridin-3-yl) phenyl)-2-phenylpyrimidine (B3pyPPM), or B3PyMPM. The device results showed that the exciplex uses B4pyMPM with high mobility and superior injection property to achieve an unprecedented PE of 136.6 lm W^{-1} and an ultra-low turn-on voltage of 2.2 V.[34] In 2017, Park *et al.* found that the lifetime of the exciplex device is related to the difference in the singlet energy level of donors and acceptors (ΔE_{DA}) and the ΔE_{ST} of exciplex. They found that the smaller the ΔE_{DA} and ΔE_{ST}, the longer the lifetime of the device.[35] Kim *et al.* used TAPC and B4PYMPM to form exciplexes, doped fluorescent emitter of 2,8-di[*t*-butyl]-5,11-di[4-(*t*-butyl) phenyl]-6,12-diphenylnaphthacene (TBRb) and phosphorescent emitter of bis(2-phenylpyridine) iridium(III)(2,2,6,6-tetramethylheptane-3,5-diketonate) ($Ir(ppy)_2tmd$), with a maximum EQE of 26.1%. Compared to the device with $Ir(ppy)_2tmd$ or TBRb, the lifetime of the codoped device with both $Ir(ppy)_2tmd$ and TBRb has been significantly improved. They found that the stability of the device depends on the position where the excited state is formed, and indicated a feasible method to achieve a long-lived high-efficiency fluorescent OLED.[36]

In 2020, Wong *et al.* studied the performance of the bulk-type BCzPh:CN-T2T and interface-type BCzPh/CN-T2T exciplex device. BCzPh is 9,9′-diphenyl-9*H*,9′*H*-3,3′-bicarbazole. The maximum EQE of the interface and the bulk-type device are respectively 7.7% and 26.4%. The emission spectrum shows that the bulk-type device only exhibits exciplex emission, while the main emission of the interface-type device comes from the CN-T2T layer, and the contribution of the exciplex emission is relatively small. Therefore, efficient and stable formation of intermolecular charge transfer states is a prerequisite for ideal device performance, which is the advantage of bulk-type exciplex.[37]

The device performance of the bulk exciplex for green emission is summarized in Table 1.

Table 1 Bulk exciplex for green emission

EML	V_{on} (V)	EQE_{max}[a] (%)	PE_{max}[b] (lm W^{-1})
m-MTDATA:PPT[20]	—	10.0	47.0
TCTA:Tm_3PyBPZ[21]	2.4	13.1	54.2
Tris-PCz:CN-T2T[22]	—	11.9	46.5
m-MTDATA:Bphen[13]	—	7.8	—
m-MTDATA:3TPYMB[26]	2.7	—	—
m-MTDATA:OXD-7[27]	—	3.8	—
13PXZB:B4PyMPM[28]	2.5	14.6	48.3
Pra-2DMAC:PO-T2T[29]	2.4	15.0	—
TAPC:DPTPCz:C545T[30]	2.8	14.5	46.1
mCP:B3PyMPM:4CzIPN[31]	3.0	29.6	—
TAPC:A4:$Ir(ppy)_3$[32]	2.4	29.6	128.2
TCTA:B3PYMPM:DACT-II[33]	—	34.2	—
CBP:B4pyPPM:DACT-II[34]	2.2	—	136.6
TAPC:B4PYMPM:TBRb:$Ir(ppy)_2tmd$[36]	2.2	26.1	114.3
BCzPh:CN-T2T[37]	2.5		26.4

[a] EQE_{max} is maximum external quantum efficiency. [b] PE_{max} is maximum power efficiency, the same below.

2.2 Bulk exciplex for red emission

The most common red emission from the exciplex host is doped with 5,6,11,12-tetraphenylnaphthacene (rubrene) or 4-(dicyanomethylene)-2-*t*-butyl-6-(1,1,7,7-tetramethyljulolidyl-9-enyl)-4*H*-pyran (DCJTB). Due to the TADF process of the exciplex host, the doped device exhibits high EQE. In 2015, the orange emitter of rubrene was doped into a 3,3-di(9*H*-carbazol-9-yl) biphenyl (mCBP):PO-T2T exciplex. To optimise the energy transfer conditions, when doping 0.4 wt% of rubrene to the exciplex host, an EQE of 6.1% was obtained; CIE coordinates were (0.3161, 0.4269), much higher than 3.9% for the pure rubrene device, indicating the effective exciton confinement of the exciplex host. The red guest material DCJTB was used to replace rubrene, and the highest EQE of 6.2% was obtained.[38] Zhang *et al.* also reported similar results, using TCTA:2,4,6-tris(3-(1*H*-pyrazol-1-yl)phenyl)-1,3,5-triazine (3P-T2T) as the host of DCJTB, with the device structure of ITO/MoO_3 (3 nm)/NPB (20 nm)/TCTA (8 nm)/TCTA : 3P-T2T (1 : 1):1 wt% DCJTB (15 nm)/3P-T2T (45 nm)/LiF/Al, CE 22.7 cd A^{-1}, PE 21.5 lm W^{-1}, EQE 10.2% were obtained, where NPB is *N*,*N*′-bis-(1-naphthl)-diphenyl-1,1′-biphenyl-4,4′-diamine. The reason for the high efficiency of the device is that the high RISC rate of the TCTA:3P-T2T system enables the efficient energy transfer from the host to the emitter.[39]

In order to further improve the efficiency of DCJTB-doped devices. Kim *et al.* used the TCTA:B4PYMPM exciplex as the host of DCJTB, and the PLQY of the exciplex film was 60%.[40] After doping with 0.5 wt% DCJTB, the overall PLQY reached 73%. They also studied the photoluminescence of the film in different directions and proved that the horizontal orientation ratio of the molecules in the film is 86%. High horizontal molecular orientation can enhance light extraction efficiency, and the device structure is as follows: ITO/TAPC (75 nm)/TCTA (10 nm)/TCTA:B4PYMPM:*x* wt% DCJTB (30 nm)/B4PYMPM (50 nm)/LiF/Al, the EQE is 10.6%, CE 20.5 cd A^{-1}, and PE 26.8 lm W^{-1}. Lately, they proposed a strategy of using a phosphorescent sensitizer to induce the exciplex to transfer

Table 2 Bulk exciplex for red emission

EML	EQE_{max} (%)	PE_{max} (lm W^{-1})
mCBP:PO-T2T:DCJTB[38]	6.2	
TCTA : 3P-T2T (1 : 1):DCJTB[39]	10.2	21.5
TCTA:B4PYMPM:DCJTB[40]	10.6	26.8
TCTA:B4PYMPM:DCJTB:Ir(ppy)$_2$(tmd)[41]	23.7	
CBP:PO-T2T:TPA-PZCN[42]	28.1	

energy to fluorescent emitters. Doping Ir(ppy)$_2$tmd in TCTA:B4-PyMPM:0.5 wt% DCJTB, with the increase in Ir(ppy)$_2$tmd concentration, the photoluminescence decay rate of the film increases, which confirms the inducing effect of Ir(ppy)$_2$tmd on the energy transfer of the exciplex to DCJTB. The device structure is as follows: ITO/TAPC (65 nm)/TCTA (10 nm)/TCTA:B4PyMPM:0.5 wt% DCJTB:*x* wt% Ir(ppy)$_2$(tmd) (30 nm)/B4PyMPM (55 nm)/LiF/Al, and the maximum EQE of 23.7% is reached with 8 wt% of phosphorescent sensitizers.[41]

In addition to doping DCJTB, in 2019, Liao *et al.* chose TPA–PZCN doped into CBP and PO-T2T cohosts. The device achieved a record EQE of 28.1% and a deep-red emission at 648 nm with the CIE coordinates of (0.66, 0.34).[42] Due to the use of the TADF material of TPA–PZCN, the utilization rate of triplet excitons is higher than that of the fluorescent material, and the device EQE can be further improved. The device performance of the bulk exciplex for red emission is summarized in Table 2.

2.3 Bulk exciplex for blue emission

Blue emission has always been the focus of recent OLED research. As an indispensable primary color in full-color displays, the performance of blue light has not been satisfactory compared to red and green light. The exciplex system also has the potential for highly efficient blue emission. In 2013, Jankus *et al.* used NPB as the donor and TPBi as the acceptor, and prepared a deep blue device structure as ITO/NPB (30 nm)/NPB:TPBi (35 nm)/TPBi (35 nm)/LiF/Al, the EQE is 2.7% at 600 cd m^{-2}, and the color coordinates are (0.15, 0.13). In the case of the NPB:TPBi exciplex, the triplet energy of NPB is lower than that of the exciplex, which is rapidly quenched by NPB, thus most of the deep blue excitons come from the TTA process of NPB.[43] Kim *et al.* also used pyrimidine core B3PyMPM as the acceptor. The PLQY of the TCTA:B3PyMPM film ranged from 36% at room temperature to 100% at 35 K, and the emission peak was at 495 nm. The device structure is ITO/TAPC (30 nm)/TCTA (10 nm)/(1 : 1) TCTA:B3PyMPM (30 nm)/B3PyMPM (20–40 nm)/LiF/Al. The EQE is 3.1% at room temperature and reaches the maximum value of 10% at 195 K.[44]

Since blue emission requires exciton with high energy, a further higher energy gap of molecules is needed to form exciplexes for blue emission. In 2013, Hung *et al.* synthesized an acceptor of 3P-T2T with triazine as the nucleus and formed an exciplex with TCTA, and the structure of the device is as follows: ITO/PEDOT:PSS (30 nm)/NPB (20 nm)/TCTA (5 nm)/TCTA:3P-T2T 50 mol% (*X* nm)/3P-T2T (75−*X* nm)/Liq/Al, where *X* = 0 or 25, *i.e.*, without/with a co-evaporated layer, the experimental results indicate that the mixed layer is conducive to higher efficiencies. The reason is that the average distance between the donor and acceptor molecules in the mixed layer is smaller, and it is easier to form a CT state.[45] The maximum EQE of the device is 7.8%, and the maximum CE is 23.6 cd A^{-1} and PE is 26.0 lm W^{-1}. In 2014, they synthesized a PO-T2T receptor with a higher LUMO energy level. The exciplex system formed with mCP and PO-T2T emitted a blue light of 472 nm, with a maximum EQE of 8%.[46] With the help of the excellent acceptor of PO-T2T, Zhang *et al.* developed a blue emission system of CDBP:PO-T2T; CDBP is 4,4′-bis(9-carbazolyl)-2,2′-dimethylbiphenyl. Because of the high E_T value of the acceptor molecule, the device with a structure of ITO/TAPC (30 nm)/CDBP (10 nm)/CDBP:50 wt% PO-T2T (30 nm)/PO-T2T (40 nm)/LiF/Al has an EQE of 13%.[47] Moreover, using PO-T2T as the acceptor, Hung *et al.* introduced a *t*-butyl group on the donor molecule to generate steric hindrance and increase the contact between the acceptor molecules. CPF (9,9-bis[4-(9-carbazolyl) phenyl] fluorene) and CPTBF (9,9-bis[4-(carbazol-9-yl) phenyl]-2,7-di*tert*-butylfluoren) were used as donors to mix with PO-T2T with a molar ratio of 1 : 1. More *t*-butyl branches make it sterically hindered, resulting in further separating adjacent excitons by a longer distance to suppress exciton–exciton annihilation. Therefore, a device with a structure of ITO/4% ReO_3:CPF (60 nm)/CPF (15 nm)/CPTBF:PO-T2T (25 nm)/PO-T2T (10 nm)/CN-T2T (40 nm)/Liq/Al increased the EQE to 12.5%, higher than 9.5% of that of the CPF:PO-T2T emitter device.[48]

Lee *et al.* used another exciplex system of TPBi and oxyboron-based compound TPAPB ((4-dimesitylboryl) phenyl-triphenylamine). The emission peak of the TPAPB : TPBi (1 : 1) co-evaporated film was at 471 nm, and the PLQY reached 44.1%. The maximum EQE of the blue exciplex device is 7%, PE is 7.2 lm W^{-1} and CE is 9.1 cd A^{-1}, with a structure of ITO/TPAPB (30 nm)/TPAPB : TPBi (1 : 1) (30 nm)/TPBi (40 nm)/LiF/Al. In addition, due to the excellent transmission properties of TPAPB and TPBi, they are also ideal exciplex as host materials.[49]

When the exciplex is used as the host doped with a blue fluorescent material, the color purity problem can be improved and deep blue emission can be obtained. Li *et al.* used TCTA and TPBi as the exciplex host, doped with a blue fluorescent diphenyl-amine-oxadiazole, PhN–OF(2)–Oxa (B2), and realized a deep blue emission prepared by the solution process. The device structure is as follows: ITO/PEDOT:PSS (35 nm)/poly (9-vinylcarbazole) (PVK) (15 nm)/EML (30 nm)/TPBi (40 nm)/Ca/Al, where the EML is spin-coated from a mixed solution of TCTA:TPBi:5 wt% B2, the maximum EQE is 3.7%, and the color coordinates are (0.167, 0.199).[50]

In addition, the exciplex as the host is advantageous to improve the charge transport performance of EML. In 2020, Zhang *et al.*[51] used spirofluorene (SF) as the π-spacer, 9-(9,9′-spirobi[fluoren]-3-yl)-9′-phenyl-9*H*,9′*H*-3,3′-bicarbazole (SFBCz) as the donor part, and 2-(3′-(9,9′-spirobi[fluoren]-3-yl)-[1,1′-biphenyl]-3-yl)-4,6-diphenyl-1,3,5-triazine (SFTRZ) as the acceptor unit, and constructed an exciplex with sky blue emission. The device showed a low turn-on voltage of 3.1 V with an EQE of 21.4% and a significant T_{80} over 8200 hours at 1000 cd m^{-2}.

Table 3 Bulk exciplex for blue emission

EML	V_{on} (V)	EQE_{max} (%)	PE_{max} (lm W^{-1})
NPB:TPBi[43]	—	2.7	—
TCTA:B3PYMPM[44]	—	3.1	—
TCTA:3P-T2T[45]	—	7.8	26.0
mCP:PO-T2T[46]	—	8.0	—
CDBP:PO-T2T[47]	—	13.0	—
CPF:PO-T2T[48]	2.2	9.5	22.9
CPTBF:PO-T2T[48]	2.2	12.5	33.2
TPAPB:TPBi[49]	3.2	7.0	5.0
TCTA:TPBi:B2[50]	—	3.7	—
SFBCz:SFTRZ:5TCzBN[51]	3.1	21.4	—
mCBP:PO-T2T:FIrpic[52]	2.6	34.1	79.6
mCBP:PO-T2T:B4PyPPM:FIrpic[53]	—	25.6	54.3
ν-DABNA:Tris-PCz:3Cz-TRZ[54]	—	19	—

In addition to the fluorescent material, the phosphorescent material bis(4,6-difluorophenylpyridinato-N, C2) picolinatoiridium (FIrpic) is also doped in the exciplex host. In 2016, Kim *et al.* demonstrated a highly efficient sky-blue phosphorescent OLED (PhOLED) with FIrpic by using an exciplex host composed of low refractive index (below 1.8) of HTL and ETL, *i.e.*, mCBP and PO-T2T, respectively. The devices show a maximum EQE of 34.1%, and a low turn-on voltage of 2.6 V with a high maximum PE of 79.6 lm W^{-1} and 65.5 lm W^{-1} at 100 cd m^{-2}, which maintained the highest EQE record of blue PhOLED.[52] Ma *et al.* created two discrete energy transmission channels in EML by introducing double excitation recombination to form a co-host. Due to the two independent energy transfer paths, the exciton energy can be more fully utilized *via* a multiple transfer mechanism compared with the single excitation structure. mCBP:PO-T2T and mCBP:B4PyPPM were chosen to be the doublet exciplex co-host for the phosphorescent FIrpic as the EML.[53]

To solve the problem of the lifetime of exciplex devices, Adachi *et al.* investigated the relationship between the unwanted carrier recombination and the TADF property of acceptors with device degradation. By employing a proposed "exciton recycling" strategy, a threefold increased operational lifetime can be achieved while still maintaining high-performance OLED properties.[54] The device performance of bulk exciplex for blue emission is summarized in Table 3.

3. Interface TADF exciplex

The bulk exciplex is usually prepared with high doping concentrations of donor and acceptor molecules, and the mixed structure is favorable to the formation of exciplex. However, mixed donors and acceptors also greatly increase the energy transfer barriers between molecules, making huge difficulty for electrons and holes to combine in the recombination region. Moreover, high doping concentration may also lead to exciton quenching, which may cause low EQE and high turn-on voltage for devices. Compared with bulk exciplexes, exciplex which formed at the interface of the donor and acceptor layers, *i.e.*, interface exciplex, can reduce the exciton quenching and enhance the radiative transition possibility. Interface exciplex can not only form between the adjacent donor and acceptor,

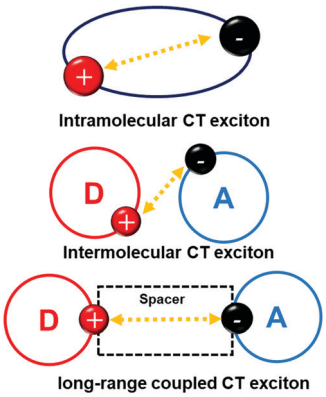

Fig. 3 Concept scheme of intramolecular CT exciton, intermolecular CT exciton and long-range coupled CT exciton.

but also between the donor and acceptor inserted by a spacer layer, as can be shown in Fig. 3. This donor/spacer/acceptor configuration enlarges the CT exciton distribution region and gives convenience to adjust the CT exciton radius, which can reduce ΔE_{ST} and improve RISC. Herein, the developments of the interface TADF exciplex (classified by emission color) are discussed and summarized systematically.

3.1 Interface exciplex for green emission

In 2015, Wang *et al.* studied the difference in the bulk and interface exciplex hosts, which consist of m-MTDATA as the donor, and TmPyPB as the acceptor.[55] They found that interfacial exciplexes show advantages including efficient charge injection and transporting, barrier-free hole–electron recombination for the formation of the exciplex and elimination of charge traps of phosphors in the EML. When doping a green–yellow phosphor emitter in the donor layer, the solution-processed device with this interface exciplex structure gave a turn-on voltage of 2.4 V and a record high PE of 97.2 lm W^{-1}.

Su *et al.* reported an interface exciplex with a simplified structure, extremely low driving voltage, and high efficiency. They used TAPC and 2,4,6-tris(3-(pyridyl) phenyl)-1,3,5-triazine (TmPyTz) to fabricate a PN-type structure. The exciton is formed at the interface of ETL and HTL without crossing the interface barrier, achieving an extremely low turn-on voltage. Besides, through harvesting singlet and triplet excitons for radiative transition simultaneously, EQE as high as 12.0% was obtained for the green and yellow OLEDs.[56]

In 2016, Sasabe *et al.* reported a high-performance green OLED based on the exciplex host formed by CBP and B4PyPPM,[57] doped with a TADF emitter of 4CzIPN. The PL spectrum of the co-evaporated film of CBP and B4pyPPM proved the formation of the exciplex. The optimized green TADF OLED showed a maximum EQE of 25.7% and a turn-on voltage of 2.3 V, which was a record of TADF OLEDs at that time.

Studies have shown that the formation of the exciplex CT state does not even require a direct contact between the donor and the acceptor because CT excitons may have a long diffusion distance. In 2016, Adachi *et al.* inserted a 10 nm spacer layer

between the donor of m-MTDATA and acceptor of 2,4,6-tris(biphenyl-3-yl)-1,3,5-triazine (T2T), and then observed long-distance coupling CT between them.[58] By adjusting the thickness of the intermediate layer, the ΔE_{ST} of the exciplex was reduced from 0.09 eV to 0.04 eV by spatially separating the donor and acceptor, increasing the ratio of delayed fluorescence. The efficiency of the green device with the intermediate layer is almost 8 times higher than that of the device without the spacer layer; this is also the first example of long-range coupled CT state between electron-donating and electron-accepting molecules in the device.

Since then, many researchers began to focus on the formation mechanism of the interface TADF exciplex. In 2018, Xu *et al.* used an external electric field to control the binding and stretching of the exciplex molecules, and explored the relationship between the recombination rate and the separation of electrons and holes. They found that the recombination rate was determined by a local process involving the lateral motion of carriers under their mutual coulombic interaction, which, in turn, was determined by the electron–hole separation, providing a more profound understanding of the basic mechanism of the efficient radiation recombination of the exciplex.[59]

In 2020, Grazulevicius *et al.* reported a novel strategy of double-channel emission from the organic exciplex coupled to fluorescence emission. The process has been demonstrated for white emission in OLEDs based on the yellow–green exciplex combined with blue fluorescence emission. Combining the fluorescence emission of m-MTDATA with the TADF exciplex emission from the DPNC/Bphen interface, a highly efficient white OLED has been fabricated. As a result, bright white OLED with 10 000 cd m^{-2} has been obtained.[60]

3.2 Interface exciplex for red emission

Usually, red emission is easier to implement than green emission. In 2016, Duan *et al.* used TCTA and (3′-(4,6-diphenyl-1,3,5-triazin-2-yl)-(1,1′-biphenyl)-3-yl)-9-carbazole (CzTrZ) to form exciplexes and doped orange phosphorescent material PO-01. They compared the results of bulk- and interface-type exciplex devices. The lifetime of the interface device is nearly 2 orders of magnitude higher than that of the device based on the bulk exciplex host. For interface-type devices, PO-01 is doped in CzTrz, and excitons are mainly generated at the interface, with a few CzTrz excitons formed, while for bulk-type devices, TCTA excitons are also formed, which is considered to be an important reason for shortening the lifetime of the device. This indicates that the interface-type exciplex has additional exciton confinement in the device.[61] In 2018, Su *et al.* also utilized long-distance radiation coupling of spatially separated electron–hole pairs to realize low driving voltage and high-efficiency exciplexes. They added a 3 nm mCP layer between TAPC doped with 1% DBP and TmPyTZ to separate electron and hole pairs, which can effectively reduce exciton relaxation and direct carrier capture by the guest material. The device achieved a maximum EQE of 14.8% with red emission.[62]

In 2019, Pu *et al.* found an exceptionally long range coupled exciplex emissions between donor and acceptor molecules even with a spacer thickness of 70 nm;[63] before then, reports about the long-range coupled CT state basically takes place in a few nanometers. Using 9,10-bis(3,5-dimethoxyphenyl) anthracene (DMA) as a spacer layer between donor TAPC and acceptor 9,10-bis(3,5-dicyanophenyl) anthracene (DCA), the red emission of exciplex keeps existing when the thickness of DMA varies from 0 to 70 nm, and they contributed this phenomenon to the exciplex formation at both the donor/spacer and the spacer/acceptor interfaces, resulting in long-distance coupling between the donor and the acceptor through such a thick spacer layer.

Besides, the interface exciplex also takes advantages in low-cost solution-processed OLEDs due to its easy fabrication method. In 2020, Huang *et al.* developed highly efficient solution-processed red PhOLEDs based on an exciplex of a NPB/TPBi-doped red phosphor bis(2-methyldibenzo[*f*,*h*]quinoxaline) (acetylacetonate) iridium(III) ($Ir(MDQ)_2(acac)$).[64] The optimal red PhOLED based on the interfacial exciplex host presents a low turn-on voltage of 2.6 V and EQE_{max} of 17.2%. They gave detailed analysis of carrier recombination pathways, which revealed the advantages of the interfacial exciplex host in carrier transport and recombination.

The exciplex can also be synergistically sensitized with phosphorescent materials. In 2018, Colella *et al.* employed an exciplex formed by 26DCzPPy and PO-T2T at the interface between the EML and the ETL to improve the stability and efficiency of PhOLED based on $Ir(dmpq)_2acac$. It shows that the presence of the TADF exciplex at the EML–ETL interface induces an efficient localization of the recombination zone, which is confined within the 5 nm–thick EML. This approach effectively improves the T_{90} of devices from $<$ 1 min to 6 h.[65] In 2020, Huang *et al.* used a phosphorescent material $Ir(ppy)_3$ doped in B3PYMPM to form an interface-type exciplex with mCP, inserting 0.2 nm C545T in the middle, to achieve ultra-thin-layered fluorescence that is synergistically sensitized by the interface exciplex and phosphorescent OLED. Due to the relatively slow FRET rate, the Dexter energy transfer (DET) between the mCP/B3PYMPM excimer and the C545T emitter dominates the mCP/C545T/B3PYMPM structure, making device performance improvements limited. With the help of phosphor, more effective FRET energy transfer paths from exciplex and/or phosphor to fluorescent molecules can be formed, achieving an EQE of 8.1%.[66]

Table 4 Interface exciplex TADF

EML	V_{on} (V)	EQE_{max} (%)	PE_{max} (lm W^{-1})	Colour
m-MTDATA:Ir(Flpy-CF_3)$_3$/TmPyPB[55]	2.4	25.2	97.2	Green
CBP/B4pyPPM:4CzIPN[57]	2.3	25.7	107	Green
m-MTDATA/mCBP/T2T[58]	—	2.8	—	Green
TAPC/TmPyTZ[56]	2.1	12.0	52.8	Yellow
TCTA/CzTrZ:PO-01[61]	3.1	27.0	73.1	Red
TAPC:DBP/TmPyTZ[62]	2.2	13.0	54.3	Red
TAPC:DBP/mCP/TmPyTZ[62]	2.2	14.8	38.8	Red
NPB/Ir(MDQ)$_2$(acac)/TPBi[64]	2.6	17.2	40.4	Red
26DCzPPy:Ir(dmpq)2acac/PO-T2T[65]	4.0	26.0		Red
mCP/C545T/B3PYMPM:Ir(ppy)$_3$[66]	3.4	8.1	25.7	Red
m-MTDATA/ADN[67]	2.2	3.8		Blue
CDBP:4CzFCN/PO-T2T[68]	3.6	21.0	46.7	Blue
DBFPO/TSPO1[69]	2.5	41.2	87.2	Blue

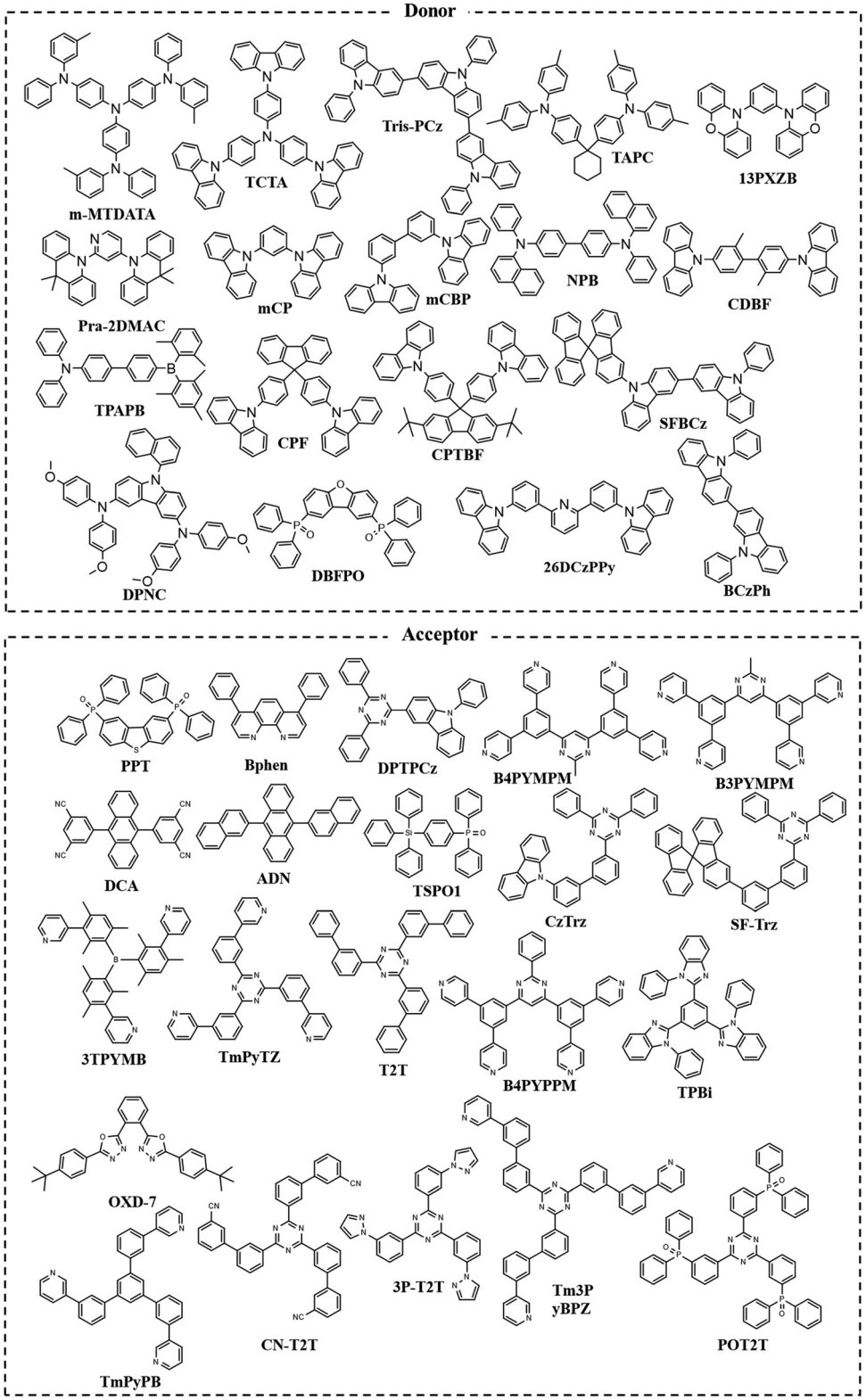

Fig. 4 Chemical structures of donor and acceptor molecules involved in this review.

3.3 Interface exciplex for blue emission

Compared with red or green emission exciplexes, blue emission requires both donors and acceptors to have higher E_T values to match, which is a challenge to the transportation and stability of the corresponding materials. In 2017, Lin *et al.* successfully constructed an up-conversion OLED based on the exciplex-sensitized TTA mechanism, which is characterized by an ultra-low sub-band gap driving voltage, for example, blue

devices only operated at 2.2 V when it turned on (the band gap is 2.9 eV). At the interface of m-MTDATA/9,10-bis(2′-naphthyl) anthracene (ADN), the triplet exciton of the exciplex is formed and captured by the lower T_1 values of ADN, and then, the TTA process of ADN is triggered to achieve high-energy blue emission ($S_1 \rightarrow S_0$). This exciplex-sensitized TTA OLED has a low drive voltage, but its EQE performance is low (0.1%) due to the quenching of the reverse energy transfer from S_1 of ADN to S_1 of the exciplex. After adding a fluorescent layer as a ''triplet diffusion and singlet barrier layer'', the corresponding EQE is dramatically improved to 3.8%.[67]

In 2019, three interfacial exciplexes were used as hosts to develop efficient blue solution–processed TADF-OLEDs by Zheng *et al.*.[68] The best configuration is based on the CDBP/PO-T2T (where CDBP is 4,4′-bis(9-carbazolyl)-2,2′-dimethyl-biphenyl) exciplex host with a soluble blue TADF emitter, which realized a blue OLED with a maximum EQE of 21.0% and a low turn-on voltage of 3.6 V. The results indicated that the interface exciplex would be a suitable host for future solution-processed TADF-OLEDs.

The interface exciplex excitons are mainly formed at the interface of donor and acceptor molecules, so that the exciton may avoid entering the low E_T material to cause quenching. In 2021, Vasilopoulou *et al.* used the DBFPO/TSPO1 interface exciplex with the highly efficient HTM T2fQ to confine the excitons at the EML/ETM interface, thereby avoiding the adverse effect of the low E_T value of HTM on the device efficiency, and the maximum EQE of the blue device reached 41.2%.[69] DBFPO is bis(diphenylphosphine oxide)dibenzofuran and TSPO1 is diphenyl[4-(triphenylsilyl) phenyl]phosphineoxide. The device performance of interface exciplexes is summarized in Table 4.

Although the interface-type exciplex requires the donor molecule to possess a strong electron blocking ability, and the acceptor molecule has a strong hole blocking ability, and thus corresponding requirements for the molecular energy level matching should be needed, it is still a more promising candidate compared with bulk exciplex. The interfacial exciplex provides energy barrier-free for charge injection and charge transport. Besides, the excitons generated by the interface-type exciplex are concentrated at the interface of the donor/acceptor molecules, and the recombination zone is about 5 nm thick, which can effectively reduce the exciton capture by transport materials, leading to a higher efficiency and better stability.

The chemical structures of donor and acceptor molecules involved in this review are summarized in Fig. 4.

4. Conclusion

In summary, the booming development of the TADF exciplex in recent years affords emerging but effective ways in designing materials for OLEDs. Nowadays, the TADF exciplex not only has comparable EL performance with state-of-the-art single TADF molecular emitters, but also can be used as highly efficient hosts for high-performance devices. The TADF exciplex emitter directly composed of HTM and ETM, which can better satisfy the charge balance and simplify the device structure to achieve lower operating voltages and higher efficiencies.

Thus far, there have been many reports on the research of high-efficiency interface and bulk TADF exciplex-type OLEDs, but we still face many challenges. From the view of colour, red and green exciplex devices have achieved sufficient efficiency and lifetime, which are close to or meet the requirements of commercialization, while blue exciplex devices still need to be further developed. Among intramolecular blue TADF emitters, it is very difficult to achieve high E_T and small ΔE_{ST} at the same time, currently only B–N narrow-band material is a promising candidate. While for intermolecular TADF, there are more choices for donors and acceptors, and high E_T can be obtained relatively easily. Combining the advantages of the interface exciplex with high-colour purity blue emitter guests, using donors and acceptors with high E_T to form the interface exciplex as the host, doped with an ultra-thin deep blue emitter, *e.g.*, B–N narrow-band material, might be a potential solution for blue emission.

Author contributions

J. G., Z. T., H. G., and Y. C. performed references analysis and manuscript writing; J. X., Z. C., and L. X. organized and inspect the manuscript.

Conflicts of interest

There are no conflicts to declare.

Acknowledgements

This work was financially supported by the National Natural Science Foundation of China (No. 61935016, 52173153, and 12174013) and the Shandong Province Key R&D Program (No. 2019GGX101016).

References

1 C. W. Tang and S. A. Vanslyke, *Appl. Phys. Lett.*, 1987, **51**, 913–915.
2 H. Sasabe and J. Kido, *Eur. J. Org. Chem.*, 2013, 7653–7663.
3 M. Y. Wong and E. Zysman-Colman, *Adv. Mater.*, 2017, **29**, 1605444.
4 J. H. Burroughes, D. D. C. Bradley, A. R. Brown, R. N. Marks, K. Mackay, R. H. Friend, P. L. Burn and A. B. Holmes, *Nature*, 1990, **347**, 539–541.
5 M. A. Baldo, D. F. O'Brien, M. E. Thompson and S. R. Forrest, *Phys. Rev. B: Condens. Matter Mater. Phys.*, 1999, **60**, 14422–14428.
6 M. A. Baldo, D. F. O'Brien, Y. You, A. Shoustikov, S. Sibley, M. E. Thompson and S. R. Forrest, *Nature*, 1998, **395**, 151–154.

7 C. Adachi, M. A. Baldo, M. E. Thompson and S. R. Forrest, *J. Appl. Phys.*, 2001, **90**, 5048–5051.
8 K.-H. Kim, C.-K. Moon, J.-H. Lee, S.-Y. Kim and J.-J. Kim, *Adv. Mater.*, 2014, **26**, 3844–3847.
9 A. Endo, M. Ogasawara, A. Takahashi, D. Yokoyama, Y. Kato and C. Adachi, *Adv. Mater.*, 2009, **21**, 4802–4806.
10 M. Kim, S. K. Jeon, S.-H. Hwang and J. Y. Lee, *Adv. Mater.*, 2016, **28**, CP9–CP9.
11 D. Zhang, M. Cai, Y. Zhang, D. Zhang and L. Duan, *Mater. Horiz.*, 2016, **3**, 145–151.
12 Y. Tao, K. Yuan, T. Chen, P. Xu, H. H. Li, R. F. Chen, C. Zheng, L. Zhang and W. Huang, *Adv. Mater.*, 2014, **26**, 7931–7958.
13 T. Hatakeyama, K. Shiren, K. Nakajima, S. Nomura, S. Nakatsuka, K. Kinoshita, J. P. Ni, Y. Ono and T. Ikuta, *Adv. Mater.*, 2016, **28**, 2777–2781.
14 J. F. Guo, Y. G. Zhen, H. L. Dong and W. P. Hu, *J. Mater. Chem. C*, 2021, **9**, 16843–16858.
15 Q. Wang, Q. S. Tian, Y. L. Zhang, X. Tang and L. S. Liao, *J. Mater. Chem. C*, 2019, **7**, 11329–11360.
16 M. Zhang, C. J. Zheng, H. Lin and S. L. Tao, *Mater. Horiz.*, 2021, **8**, 401–425.
17 B. H. Zhang and Z. Y. Xie, *Front. Chem.*, 2019, **7**, 00306.
18 M. Sarma and K. T. Wong, *ACS Appl. Mater. Interfaces*, 2018, **10**, 19279–19304.
19 F. B. Dias, T. J. Penfold and A. P. Monkman, *Methods Appl. Fluoresc.*, 2017, **5**, 012001.
20 K. Goushi, K. Yoshida, K. Sato and C. Adachi, *Nat. Photonics*, 2012, **6**, 253–258.
21 L. Zhang, C. Cai, K. F. Li, H. L. Tam, K. L. Chan and K. W. Cheah, *ACS Appl. Mater. Interfaces*, 2015, **7**, 24983–24986.
22 W. Y. Hung, P. Y. Chiang, S. W. Lin, W. C. Tang, Y. T. Chen, S. H. Liu, P. T. Chou, Y. T. Hung and K. T. Wong, *ACS Appl. Mater. Interfaces*, 2016, **8**, 4811–4818.
23 T. Y. Zhang, B. Chu, W. L. Li, Z. S. Su, Q. M. Peng, B. Zhao, Y. S. Luo, F. M. Jin, X. W. Yan, Y. Gao, H. R. Wu, F. Zhang, D. Fan and J. B. Wang, *ACS Appl. Mater. Interfaces*, 2014, **6**, 11907–11914.
24 X. K. Liu, Z. Chen, C. J. Zheng, C. L. Liu, C. S. Lee, F. Li, X. M. Ou and X. H. Zhang, *Adv. Mater.*, 2015, **27**, 2378–2383.
25 P. L. dos Santos, F. B. Dias and A. P. Monkman, *J. Phys. Chem. C*, 2016, **120**, 18259–18267.
26 H. A. Al Attar and A. P. Monkman, *Adv. Mater.*, 2016, **28**, 8014–8020.
27 L. Song, Y. S. Hu, Z. Q. Liu, Y. Lv, X. Y. Guo and X. Y. Liu, *ACS Appl. Mater. Interfaces*, 2017, **9**, 2711–2719.
28 M. Zhang, C. J. Zheng, K. Wang, Y. Z. Shi, D. Q. Wang, X. Li, H. Lin, S. L. Tao and X. H. Zhang, *Adv. Funct. Mater.*, 2021, **31**, 2010100.
29 N. Zhang, C. J. Zheng, Z. P. Chen, J. W. Zhao, M. Zhang, H. Y. Yang, Z. Y. He, X. Y. Du and S. L. Tao, *J. Mater. Chem. C*, 2021, **9**, 600–608.
30 X. K. Liu, Z. Chen, C. J. Zheng, M. Chen, W. Liu, X. H. Zhang and C. S. Lee, *Adv. Mater.*, 2015, **27**, 2025–2030.
31 J. W. Sun, J. H. Lee, C. K. Moon, K. H. Kim, H. Shin and J. J. Kim, *Adv. Mater.*, 2014, **26**, 5684–5688.
32 B. Y. Liang, J. X. Wang, Y. Y. Cui, J. B. Wei and Y. Wang, *J. Mater. Chem. C*, 2020, **8**, 2700–2708.
33 C. K. Moon, K. Suzuki, K. Shizu, C. Adachi, H. Kaji and J. J. Kim, *Adv. Mater.*, 2017, **29**, 1606448.
34 H. Sasabe, R. Sato, K. Suzuki, Y. Watanabe, C. Adachi, H. Kaji and J. Kido, *Adv. Opt. Mater.*, 2018, **6**, 1800376.
35 S. Lee, H. Koo, O. Kwon, Y. J. Park, H. Choi, K. Lee, B. Ahn and Y. M. Park, *Sci. Rep.*, 2017, **7**, 11995.
36 H. G. Kim, K. H. Kim and J. J. Kim, *Adv. Mater.*, 2017, **29**, 1702159.
37 N. R. Al Amin, K. K. Kesavan, S. Biring, C. C. Lee, T. H. Yeh, T. Y. Ko, S. W. Liu and K. T. Wong, *ACS Appl. Electron. Mater.*, 2020, **2**, 1011–1019.
38 T. Y. Zhang, B. Zhao, B. Chu, W. L. Li, Z. S. Su, X. W. Yan, C. Y. Liu, H. R. Wu, Y. Gao, F. M. Jin and F. H. Hou, *Sci. Rep.*, 2015, **5**, 10234.
39 B. Zhao, T. Y. Zhang, B. Chu, W. L. Li, Z. S. Su, H. R. Wu, X. W. Yan, F. M. Jin, Y. Gao and C. Y. Liu, *Sci. Rep.*, 2015, **5**, 10697.
40 K. H. Kim, C. K. Moon, J. W. Sun, B. Sim and J. J. Kim, *Adv. Opt. Mater.*, 2015, **3**, 895–899.
41 H. G. Kim, K. H. Kim, C. K. Moon and J. J. Kim, *Adv. Opt. Mater.*, 2017, **5**, 1600749.
42 Y. L. Zhang, Q. Ran, Q. Wang, Y. Liu, C. Hanisch, S. Reineke, J. Fan and L. S. Liao, *Adv. Mater.*, 2019, **31**, 1902368.
43 V. Jankus, C. J. Chiang, F. Dias and A. P. Monkman, *Adv. Mater.*, 2013, **25**, 1455–1459.
44 Y. S. Park, K. H. Kim and J. J. Kim, *Appl. Phys. Lett.*, 2013, **102**, 153306.
45 W. Y. Hung, G. C. Fang, Y. C. Chang, T. Y. Kuo, P. T. Chou, S. W. Lin and K. T. Wong, *ACS Appl. Mater. Interfaces*, 2013, **5**, 6826–6831.
46 W. Y. Hung, G. C. Fang, S. W. Lin, S. H. Cheng, K. T. Wong, T. Y. Kuo and P. T. Chou, *Sci. Rep.*, 2014, **4**, 5161.
47 X. K. Liu, Z. Chen, J. Qing, W. J. Zhang, B. Wu, H. L. Tam, F. R. Zhu, X. H. Zhang and C. S. Lee, *Adv. Mater.*, 2015, **27**, 7079–7085.
48 W. Y. Hung, T. C. Wang, P. Y. Chiang, B. J. Peng and K. T. Wong, *ACS Appl. Mater. Interfaces*, 2017, **9**, 7355–7361.
49 Z. Chen, X. K. Liu, C. J. Zheng, J. Ye, C. L. Liu, F. Li, X. M. Ou, C. S. Lee and X. H. Zhang, *Chem. Mater.*, 2015, **27**, 5206–5211.
50 J. H. Peng, X. J. Xu, X. J. Feng and L. D. Li, *J. Lumin.*, 2018, **198**, 19–23.
51 C. Zhang, Y. Lu, Z. Y. Liu, Y. W. Zhang, X. W. Wang, D. D. Zhang and L. Duan, *Adv. Mater.*, 2020, **32**, 2004040.
52 H. Shin, J. H. Lee, C. K. Moon, J. S. Huh, B. Sim and J. J. Kim, *Adv. Mater.*, 2016, **28**, 4920–4925.
53 T. M. Zhang, J. W. Yao, S. Zhang, S. Xiao, W. Liu, Z. B. Wu and D. G. Ma, *J. Mater. Chem. C*, 2021, **9**, 6062–6067.
54 T. B. Nguyen, H. Nakanotani, T. Hatakeyama and C. Adachi, *Adv. Mater.*, 2020, **32**, 1906614.
55 S. M. Wang, X. D. Wang, B. Yao, B. H. Zhang, J. Q. Ding, Z. Y. Xie and L. X. Wang, *Sci. Rep.*, 2015, **5**, 12487.
56 D. C. Chen, G. Z. Xie, X. Y. Cai, M. Liu, Y. Cao and S. J. Su, *Adv. Mater.*, 2016, **28**, 239–244.

57 Y. Seino, S. Inomata, H. Sasabe, Y. J. Pu and J. Kido, *Adv. Mater.*, 2016, **28**, 2638–2643.
58 H. Nakanotani, T. Furukawa, K. Morimoto and C. Adachi, *Sci. Adv.*, 2016, **2**, 150147.
59 Q. Y. Huang, S. L. Zhao, P. Wang, Z. L. Qin, Z. Xu, D. D. Song, B. Qiao and X. R. Xu, *J. Lumin.*, 2018, **201**, 38–43.
60 K. Ivaniuk, P. Stakhira, I. Helzhynskyy, S. Kutsiy, Z. Hotra, T. Deksnys, D. Volyniuk, J. Grazulevicius and V. Gorbulic, *IEEE 15th International Conference on Advanced Trends in Radioelectronics, Telecommunications and Computer Engineering (TCSET)*, 2020, 821–824.
61 D. D. Zhang, M. H. Cai, Y. G. Zhang, Z. Y. Bin, D. Q. Zhang and L. Duan, *ACS Appl. Mater. Interfaces*, 2016, **8**, 3825–3832.
62 B. B. Li, L. Gan, X. Y. Cai, X. L. Li, Z. H. Wang, K. Gao, D. C. Chen, Y. Cao and S. J. Su, *Adv. Mater. Interfaces*, 2018, **5**, 1800025.
63 Y. J. Pu, Y. Koyama, D. Otsuki, M. Kim, H. Chubachi, Y. Seino, K. Enomoto and N. Aizawa, *Chem. Sci.*, 2019, **10**, 9203–9208.
64 J. Wang, X. L. Zhang, L. X. Fan, X. L. Zhang, Y. Qin, R. Q. Li, Y. H. Chen, W. Y. Lai, X. W. Zhang and W. Huang, *J. Mater. Chem. C*, 2020, **8**, 9909–9915.
65 M. Colella, P. Pander, D. D. Pereira and A. P. Monkman, *ACS Appl. Mater. Interfaces*, 2018, **10**, 40001–40007.
66 M. G. Li, Y. Z. Dai, Y. Zhang, J. Wang, Y. Tao, C. Zheng, R. F. Chen and W. Huang, *ACS Appl. Electron. Mater.*, 2020, **2**, 3704–3710.
67 B. Y. Lin, C. J. Easley, C. H. Chen, P. C. Tseng, M. Z. Lee, P. H. Sher, J. K. Wang, T. L. Chiu, C. F. Lin, C. J. Bardeen and J. H. Lee, *ACS Appl. Mater. Interfaces*, 2017, **9**, 10963–10970.
68 Z. Y. He, C. Y. Wang, J. W. Zhao, X. Y. Du, H. Y. Yang, P. L. Zhong, C. J. Zheng, H. Lin, S. L. Tao and X. H. Zhang, *J. Mater. Chem. C*, 2019, **7**, 11806–11812.
69 M. Vasilopoulou, A. R. B. Yusoff, M. Daboczi, J. Conforto, A. E. X. Gavim, W. J. da Silva, A. G. Macedo, A. Soultati, G. Pistolis, F. K. Schneider, Y. F. Dong, P. Jacoutot, G. Rotas, J. Jang, G. C. Vougioukalakis, C. L. Chochos, J. S. Kim and N. Gasparini, *Nat. Commun.*, 2021, **12**, 4868.

